ASSESSING THE EFFECTS OF INHERITED MUTATIONS ON PALB2 STRUCTURE AND FUNCTION

By

Davis Martin

Submitted in partial fulfillment of the

requirements for Departmental Honors in

the Department of Biology

Texas Christian University

Fort Worth, Texas

May 3, 2021

ASSESSING THE EFFECTS OF INHERITED MUTATIONS ON PALB2 STRUCTURE AND FUNCTION

Project Approved:

Supervising Professor: Mikaela Stewart, Ph.D.

Department of Biology

Giri Akkaraju, Ph.D.

Department of Biology

Sergei Dzyuba, Ph.D

Department of Chemistry and Biochemistry

ABSTRACT

The proper functioning of the protein PALB2 is vital to preventing tumor formation within breast tissues in individuals. Upon the detection of DNA damage, PALB2 and BRCA1 bind to each other along with BRCA2 to form a DNA repair complex. This complex then repairs DNA double-strand breaks in order to prevent the accumulation of DNA damage that leads to breast cancer. While both BRCA1 and BRCA2 have been extensively studied, a lot of information about the structure and function of PALB2 remains unknown. It is thought that BRCA1 and PALB2 bind via PALB2's coiled-coil domain; however, how variants of unknown significance (VUS) affect this binding interaction is largely unknown. Further, while some of these VUS have been studied *in vivo*, cheaper and easier *in vitro* methods to measure their effect on binding affinity have yet to be formulated. Thus, we hypothesized that isothermal titration calorimetry (ITC) could be used as an *in vitro* testing method for assessing the effects of VUS within the coiled-coil domain of PALB2 on the binding event between PALB2 and BRCA1. Further, we hypothesized that a decrease in binding between the two proteins as measured by ITC would correlate with a decrease in DNA repair as measured *in vivo*. We tested the efficacy of this method by creating seven mutations within the coiled-coil domain of PALB2 and measuring the binding event of PALB2 to BRCA1 via ITC. Our results strongly suggest that the binding event is enthalpic in nature and can be adequately measured using ITC as evidenced by the correlation between our *in vitro* data and previous *in vivo* data.

ACKNOWLEDGEMENTS

I would like to thank Dr. Stewart most of all for her continued support, mentorship, and patience with me as I learned how to become a real scientist during this project. Her continued support of this project was essential to its initiation and completion, and I cannot thank her enough for all of her time and energy. In addition, I would like to thank all the lab members of the Stewart lab for assisting me throughout this process either through your friendship or your assistance with my work. Thank you to Christine, Ishor, Russell, Brian, Jane, and all the other members of the lab. In addition, thank you to Peyton, Ryal, Cage, Jake, and Mary for your support and encouragement as I undertook this project; your kindness and friendship kept me motivated until the end. In addition, I want to thank my family for their love and support throughout my life and especially during these last four years. Without you, I would have none of the opportunities I currently enjoy. Lastly, I want to thank the TCU College of Science and Engineering for providing the funding and resources to make this project possible, and my committee members—Dr. Akkaraju and Dr. Dzyuba—for their time and feedback on this thesis. Without all of these people, I would not have been able to complete this work.

TABLE OF CONTENTS

INTRODUCTION

Breast cancer is one of the most common cancers among women in the United States, second only to some skin cancers, with more than 200,000 new cases diagnosed in the United States each year.[1] While the breast cancer incidence rate has remained fairly constant over the last decade, the death rate has seen a slight decrease when adjusted for population changes.[1] One of the major reasons for this decrease in breast cancer associated fatalities has been increases in medical knowledge and technologies such as the connection between genetic mutations and tumorigenesis. While Dr. Mary-Claire King first cemented this link with the discovery of the *BRCA1* gene in 1990, mutations in multiple other genes have also been implicated as increasing a woman's chance of developing breast cancer.[2] While each of these genes encodes for different proteins, many of them are all a part of a category of proteins called tumor suppressor proteins.

Tumor suppressor proteins—due to their ability to fix DNA damage and prevent uncontrollable cell growth— are the body's number one defense against tumor formation (tumorigenesis). There are a multitude of tumor suppressor proteins; however, within breast tissues, BRCA1 is one of the most prominent. Along with its accessory proteins PALB2 and BRCA2, BRCA1 is responsible for repairing double strand breaks within the DNA to prevent tumorigenesis.[3-7]

These double strand breaks are often caused by gamma irradiation damage. Once the break occurs, certain genes can be disrupted, and a cell's ability to live and replicate can be jeopardized. However, the presence of this break in the backbone of the DNA triggers the activity of BRCA1.[7] Once activated, BRCA1 binds to PALB2 to form a heterodimer complex, which in turn binds to the BRCA2 protein to complete the complex necessary for fixing the DNA break via a process called homologous recombination (figure 1). If the cell loses the ability to fix

these breaks in the DNA, it can slowly garner all the DNA damage needed to cause aberrant cell growth, resulting in tumor formation.[8] Thus, the proper functioning of these proteins is essential to the success of the cell and the prevention of tumor growth.

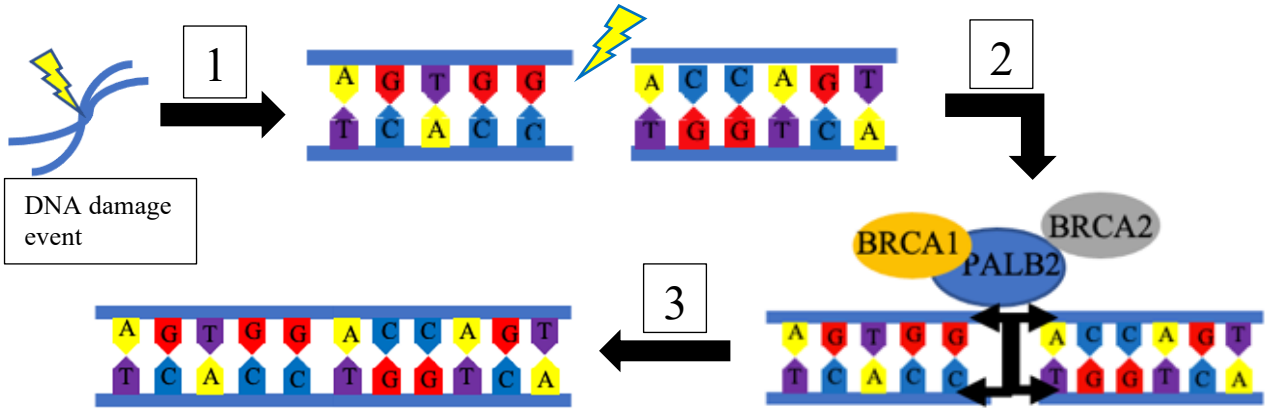

Figure 1. PALB2 forms a heterotrimer complex with BRCA1 and BRCA2 in order to fix double strand breaks in DNA via homologous recombination.[3, 7] 1. Gamma irradiation causes a double-strand break (DSB) in the DNA. 2. The DSB causes the activation and recruitment of PALB2, BRCA1, and BRCA2 to the site of the break. 3. PALB2 acts as a linker to form a heterotrimer complex with BRCA1 and BRCA2 to repair the DSB in the DNA.

Thus, it can be reasonably inferred that mutations—whether inherited or accumulated— that affect the proper functioning of these proteins could lead to an increased chance of developing breast cancer. In fact, previous literature has shown that mutations that affect the BRCA1-PALB2 interaction can lead to decreased homologous recombination efficiency and breakdowns in the cell cycle checkpoints that prevent aberrant cell growth.[3, 5, 9] Further, both of these effects are known to increase the chances for pathogenic tumor formation.[8]

Within this DNA repair complex, BRCA1 and BRCA2 have been extensively studied and evaluated for their tumorigenic potential; however, mutations within the protein PALB2 have only been recently identified as being tumorigenic.[9] Due to the relatively small amount of current knowledge about the structure and functions of PALB2, we chose to focus specifically on this protein.

While mutations within the PALB2 protein have been linked to increased tumorigenicity, these mutations are largely found in two main regions of the protein which are important for its function.[6] The first region is found near the C-terminal side of the protein and is responsible for binding to BRCA2 in order to form the HR repair complex (figure 2). This region is termed the WD40 domain, and previous literature has found that mutations within this region can be detrimental to proper protein function.[6] While the structure and function of the WD40 domain have been described extensively, the second binding domain on PALB2 that is responsible for its binding to BRCA1 lacks the same in-depth understanding.[3, 4] The structure of this domain has been elucidated (Figure 2b); however, the exact binding interface formed with BRCA1 remains unclear.[4] Without a known binding interface between the proteins, it is difficult to determine which inherited mutations are actually detrimental to the function of PALB2 and possibly cancerous. For this reason, we chose to focus on mutations within the BRCA1 binding domain on PALB2.

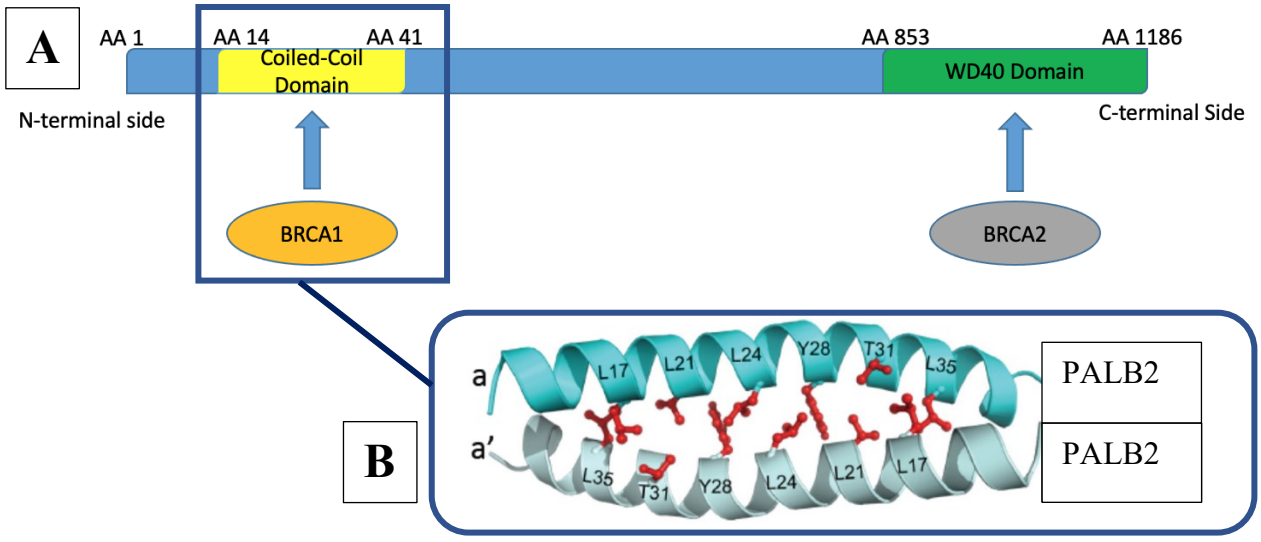

Figure 2. PALB2 binds BRCA2 via its WD40 domain (AA 853-1186), and it binds BRCA1 via its coiled-coil domain (AA 14-41).[3, 4] (a) The structure of PALB2 and its relevant binding domains are shown as well as the associated proteins that bind to these functional domains. (b) The predicted binding interface between two PALB2 monomers to form the PALB2 homodimer complex. This binding interface is also thought to be used by BRCA1 to bind to PALB2.

When analyzing the BRCA1 binding domain on PALB2, it was found that it is known to contain a conserved coiled-coil motif that homodimerizes with another PALB2 protein in order to stabilize the region when inactive.[4] It is thought that this homodimerization might play an important role in regulating the HR activity of PALB2; however, more research needs to be done to confirm this.[4, 7] Upon binding, it is thought that BRCA1 outcompetes the homodimer structure to bind to one of the two PALB2 monomers.[3-5] The specific amino acids within the PALB2 coiled-coil domain used for binding have been narrowed to a small stretch between the residues 14-41. Within this region, a plethora of mutations have been recorded in individuals with a family history of breast cancer; however, it is not known what the true effects of these mutations are on PALB2's function.[9] We refer to these mutations as variants of unknown significance (VUS) because it needs to be experimentally determined whether they actually lead to a loss of function when present in PALB2. Previous studies have attempted to identify which of these VUS cause loss of function upon induced mutations; however, all of these studies fail to focus directly on binding or structural data. Instead, the studies focus on measuring changes in HR efficiency within cells[5, 9, 10]. This data tells us that PALB2 loses some amount of function; however, it fails to tell us why it loses that function. A method that directly analyzes the effects of these mutations on the binding interaction with BRCA1 provides a clearer answer to this question. Thus, we hoped to develop a new *in vitro* method for assessing the effects of these VUS on the binding interaction between PALB2 and BRCA1 in order to better predict whether these mutations might be cancerous when inherited by individuals.

To accomplish this goal, we analyzed a database of known mutations that have been inherited by individuals with a family history of breast cancer and selected seven different mutations to create within this targeted range of amino acids on PALB2 (20-40). While most

targeted residues that are thought to be involved in the binding interaction, others targeted residues thought to be outside the interface. The ability for these mutants to bind to BRCA1 was then measured using the *in vitro* method, isothermal titration calorimetry (ITC). This unique testing method not only illuminates when PALB2 loses the ability to bind to BRCA1, but it also allows minute changes in binding affinity or thermodynamics to be recorded. We hypothesized that decreases in binding affinity as measured by ITC would correlate with decreases in HR efficiency in previously reported data, suggesting that ITC is a viable method for determining the effects of VUS on PALB2's function. In addition, we hoped to classify some of these VUS as either detrimental or benign to PALB2's function, giving deeper insight into whether patients that inherit these mutations might have an increased chance for developing breast cancer in their lifetime.

METHODS

Mutagenesis

Mutagenesis was performed on a plasmid containing the first 56 amino acids of the human PALB2 protein in the pET-SUMO 6xHis vector. This construct was employed to create seven different plasmids, each containing one inherited mutation found in breast cancer patients. The mutations were made with site-directed mutagenesis using DNA primers to replace the wild-type codons for each desired new codon (table 1). The mutagenic primers were then used to create plasmids that coded for the human PALB2 protein that contained the desired mutations. This process was done according to the fidelity hot start Q5 polymerase (New England Biolabs) protocol in a thermal cycler. The annealing temperatures for PCR varied by specific mutation (table 1). The plasmid was amplified by either the forward or reverse primer and then their products were annealed together in a single tube according to a previous study.[1] After obtaining

the DNA mutagenesis products, they were digested using the DpnI enzyme at 37 °C for two hours. The DpnI enzyme was used because it targets methylated DNA only, so it is able to cut up the parent plasmid leaving plasmids created in the thermocycler with the associated mutations intact. The digested human DNA plasmids were then transformed into DH5α *E. coli* competent cells using a heat shock of 45 seconds at 42 °C. After, the bacterial cells transformed with the human PALB2 plasmids were placed in 300 µL of super optimal broth with catabolite repression (SOC medium) and grown onto Luria-Bertani Broth (LB broth) agar plates containing 100 µg/mL kanamycin. The plates were incubated overnight at 37 °C and a single colony was chosen from each of the seven specific mutations. These colonies were then grown in 5 mL of LB broth for 14-16 hours in a 37 °C incubator shaking at 250 rpm. After the growth period, the plasmids were purified from the *E. coli* following the Qiagen mini-prep protocol. These purified DNA samples were then sequenced to ensure they contained the desired mutations as often the Dpn1 digestion process is not complete and wild-type colonies are purified instead. Dideoxy sequencing using the Hitachi 3130 XL Genetic Analyzer was completed using one of the two primers that annealed to the plasmid outside of the PALB2 gene region (SUMO forward or reverse, Table 1).

Primer Name	**Annealing Temperature (°C)**	**Sequence**
PALB2 F_Y28C	58	5’ CATTCTTGAAAAGGGAATGCAGCAAGACACTAGCCC3’
PALB2 R_Y28C		5’ GGGCTAGTGTCTTGCTGCATTCCCTTTTCAAGAATG 3’
PALB2 F_K30N		5’ GAAAAGGGAATACAGCAATACACTAGCCCGCCTTCAG 3’

PALB2 R_K30N	62	5’ CTGAAGGCGGGCTAGTGTATTGCTGTATTCCCTTTTC 3’
PALB2 F_R37H	58	5’ CACTAGCCCGCCTTCAGCATGCCCAAAGAGCTGAAAAG 3’
PALB2 R_R37H		5’ CTTTTCAGCTCTTTGGGCATGCTGAAGGCGGGCTAGTG 3’
PALB2 F_L24S	61	5’ GGAGAAATTAGCATTCAGCAAAAGGGAATACAGCAAGAC 3’
PALB2 R_L24S		5’ GTCTTGCTGTATTCCCTTTTGCTGAATGCTAATTTCTCC 3’
PALB2 F_L24F	62	5’ AGGAGAAATTAGCATTCTTTAAAAGGGAATACAGC 3’
PALB2 R_L24F		5’ GCTGTATTCCCTTTTAAAGAATGCTAATTTCTCCT 3’
PALB2 F_L21S	60	5’ GGAAAAGTTAAAGGAGAAATCAGCATTCTTGAAAAGGG 3’
PALB2 R_L21S		5’ CCCTTTTCAAGAATGCTGATTTCTCCTTTAACTTTTCC 3’
PALB2 F_L35P	58	5’ GACACTAGCCCGCCCGCAGCGTGCCCAAAG 3’
PALB2 R_L35P		5’ CTTTGGGCACGCTGCGGGCGGGCTAGTGTC 3’
SUMO FORWARD	50	5’ GGACTCCTTAAGATTCTTGTACGACGG 3’
SUMO REVERSE		5’ CGAATCTAGAGCCTGCAGTCTCGAGATC 3’

Table 1. Primer sequences and annealing temperatures. The nucleotides highlighted in red indicate the mutations created in order to produce the desired amino acids in the respective PALB2 protein constructs. SUMO primers were used for sequencing.

Protein Expression and Purification

After the sequencing of the human mutagenic PALB2 pET-SUMO plasmids confirmed the presence of each of the desired mutations, the plasmids for each mutation were transformed separately into BL21(DE3) competent *E. coli* cells using a heat shock of 30 seconds at 42 °C. The cells were plated on LB agar plates containing 50 µg/mL kanamycin and grown for 14-16

hours at 37 °C. After, the colonies from the plate were resuspended in 1-2 mL of LB broth before being added to 1 L of LB broth and 50 μg/mL kanamycin. The colonies were grown at 37°C shaking at 250 rpm until they reached optical density (OD) 0.6. Once OD 0.6 was reached, they were induced with 0.2 mM IPTG for 4 hours at 25 °C, shaking at 250 rpm. After 4 hours, the 1 L cultures were removed from the shaker and centrifuged in 1 L centrifuge bottles at 3000 rpm for 15 minutes at 4 °C. The centrifugation resulted in a cell pellet which was separated from the rest of the LB broth and then resuspended in a 25 mL mixture of buffer A (0.5 M NaCl, 20 mM TRIS, 5 mM imidazole, pH 7.4). The subsequent cell suspensions were then frozen at -80 °C until purification. This process was repeated seven times for each of the mutants. In addition, a 56 amino acid segment of the wild-type human PALB2 protein (WT PALB2) and a 50 amino acid segment of BRCA1 ranging from amino acids Ser-1377 to Glu-1426 (WT BRCA1) were also grown in the same manner as listed above for controls.

To begin purification of the cell suspensions, the suspensions were removed from the -80 °C freezer and thawed in a bucket of room temperature water. Throughout the thawing process, the suspension was treated with 0.1 mg/mL of egg lysozyme, bovine DNase I (Goldbio), and general use protease inhibitor cocktail (AMRESCO) according to manufacturer instructions. After thawing, the suspension was transferred to a 50 mL beaker for lysis on ice using the Vibra Cell sonicator (Sonics) (15 seconds on, 30 seconds off, 85% amplitude for a total of 10 minutes of pulse time). After lysis, the lysate was centrifuged at 14000 rpm, 4 °C for 25 minutes, effectively separating the insoluble cell debris found in the pellet from the soluble cellular proteins. The pellet of cell debris was then discarded, and the lysate was transferred to a 50 mL conical tube to be loaded into the Äkta Start GE system for purification. The PALB2 proteins were isolated from the rest of the lysate by cobalt affinity column purification using the His-Trap TALON column

(GE healthcare) following the provided manufacturer protocol. The process utilized the ability for the His tag (six histidine sequence) on SUMO located before the PALB2 mutagenic protein sequence to stick to the cobalt column while the rest of the lysate proteins flowed through unaffected. After, the protein was eluted from the column via increasing concentrations of imidazole outcompeting the His tag for binding sites on the column. The fractions that contained the PALB2 proteins were identified by absorbance readings at 280 nm measured by the Äkta system itself and combined into one conical tube.

Dialysis

Those fractions were then dialyzed overnight into a buffer containing 25 mM $NaPO_4$, 150 mM NaCl, and 1 mM DTT at pH 7. The next day, the proteins were removed from the buffer and a sample was taken for SDS-PAGE. Next, it was mixed with HRV3C (Human Rhinovirus type 14 3C) protease for 1-2 hours to allow cleavage of the His-SUMO tag. Again, a sample was taken for SDS-PAGE. Next, the proteins were run through both glutathione and nickel affinity columns which removed both glutathione (GST)-tagged HRV3C protease and His-tagged SUMO, respectively. While these stuck to the columns, cleaved PALB2 flowed through and was captured in three separate fractions of increasing imidazole concentrations. Samples of all three fractions were collected and run on a SDS-PAGE gel (along with all previously taken samples) to determine the presence and purity of the PALB2 proteins. The fractions containing the mutants of interest were then dialyzed overnight in a 4 L ITC buffer consisting of 25 mM $NaPO_4$, 50 mM NaCl buffer at pH 6.5. This process was repeated for each of the seven mutagenic PALB2 proteins as well as the WT PALB2 protein. The WT BRCA1 construct underwent all of the above procedures, however, it was also further purified via gel filtration chromatography on

the NGC Quest 10 plus chromatography system (Biorad). The Sephacryl S-100 High Resolution column (GE) was used according to manufacturer directions. This 3rd purification was performed to ensure maximum purity for an accurate concentration reading upon measurement via the BCA protein analysis assay.

Concentration of the Proteins for ITC testing

The following day the proteins were concentrated in 3,000 Dalton cut-off concentrators (PALL). The protein was centrifuged in the concentrators at 3000 rpm for 15-minute cycles until the concentration reached an acceptable value for future ITC testing. The concentrations of the proteins were recorded using the Nanodrop 1000 machine to measure the absorbance at 280 nm and the extinction coefficient of 1.49. This process was repeated for each of the seven mutants and the WT PALB2. However, the concentration of the WT BRCA1 was measured via the Thermo Scientific BCA protein analysis assay due to its inability to be measured via the Nanodrop 1000 because it does not contain any residues that absorb at 280 nm.

Sample preparation

As stated above, the samples were dialyzed into ITC buffer (24 mM $NaPO_4$, 50 mM NaCl, pH 6.5) before data collection. In addition, they were spun down to remove any undissolved protein and their concentration was verified.

ITC

Before titrations were run on any protein samples, extensive cleaning was performed on the machine in order to clear it of any contaminants. This was found to be an issue with collecting

reliable data in the past. The machine was cleaned using a combination of water into water titrations as well as ITC buffer into ITC buffer titrations. In addition, SDS runs were conducted in between water runs to further clear the machine of possible contaminants. Once these runs were completed, a single protein titration was conducted. After each titration, the syringe was cleaned by manually filling it with water and ejecting the contents followed by manually filling it with ITC buffer and ejecting. In addition, both cells were cleaned by removing the contents with a Hamilton syringe and then filling them multiple times with water and removing it. During this step, the ITC syringe was also dipped into the water in the main ITC cell in order to clean the outside of the syringe. This manual process was conducted between each run of the same mutation or protein. Whenever switching to a new protein or mutant, instrument cleanliness was

ITC RUN PARAMETERS FOR WT PALB2 AND L35P PALB2			
Experimental Parameters		**Injection Parameters**	
Total # of Injections	16	**Volume (µL)**	2
Cell Temperature (°C)	25	**Duration (sec.)**	4
Reference Power (µCal/sec)	4	**Spacing (sec.)**	250
Initial Delay (sec)	600	**Filter Period (sec.)**	5
Syringe Concentration (mM)	0.425 mM		
Cell Concentration (mM)	Varied (Table 3)		
Stirring Speed (rpm)	300		

Table 2a. ITC Settings. Listed above are the settings used to carry out ITC runs for each mutant. The concentrations of the samples varied based on the run, and the specific concentrations for each run can be found in Table 3.

verified by running a water into water titration as well as an ITC buffer into ITC buffer titration. The manual cleaning process previously described was also conducted when switching from one protein to another to further avoid cross contamination. Each of the PALB2 mutations were run at unique concentrations in order to obtain the best binding curve; however, the WT BRCA1 construct was titrated at 0.425 mM in each run. The rest of the settings used for each run can be found in the table below. The settings were changed for two of the mutations because it was difficult to obtain proper titration curves. Those changes are recorded in table 2.

ITC RUN PARAMETERS FOR L24F PALB2 AND K30N PALB2			
Experimental Parameters		**Injection Parameters**	
Total # of Injections	32	**Volume (µL)**	1
Cell Temperature (°C)	25	**Duration (sec.)**	4
Reference Power (µCal/sec)	4	**Spacing (sec.)**	250
Initial Delay (sec)	600	**Filter Period (sec.)**	5
Syringe Concentration (mM)	0.425 mM		
Cell Concentration (mM)	Varied (Table 3)		
Stirring Speed (rpm)	300		

Table 2b. ITC Settings. Listed above are the settings used to carry out ITC runs for each mutant. The concentrations of the samples varied based on the run, and the specific concentrations for each run can be found in Table 3.

Protein	WT PALB2	L35P	L24F	K30N
Concentration	0.050 mM	0.050 mM	0.075 mM	0.075 mM

Table 3. ITC Settings. Listed above are the concentrations at which each protein's final titration data was recorded at. Multiple concentrations were attempted for each protein until the best titration curve was achieved. The remaining mutations never returned usable titration curves, and thus, have been omitted from this table.

RESULTS

After the creation of the PALB2 mutant protein constructs, all of them were sequenced to confirm the presence of the proper mutation before testing for their ability to bind to the BRCA1 protein using isothermal titration calorimetry (ITC).

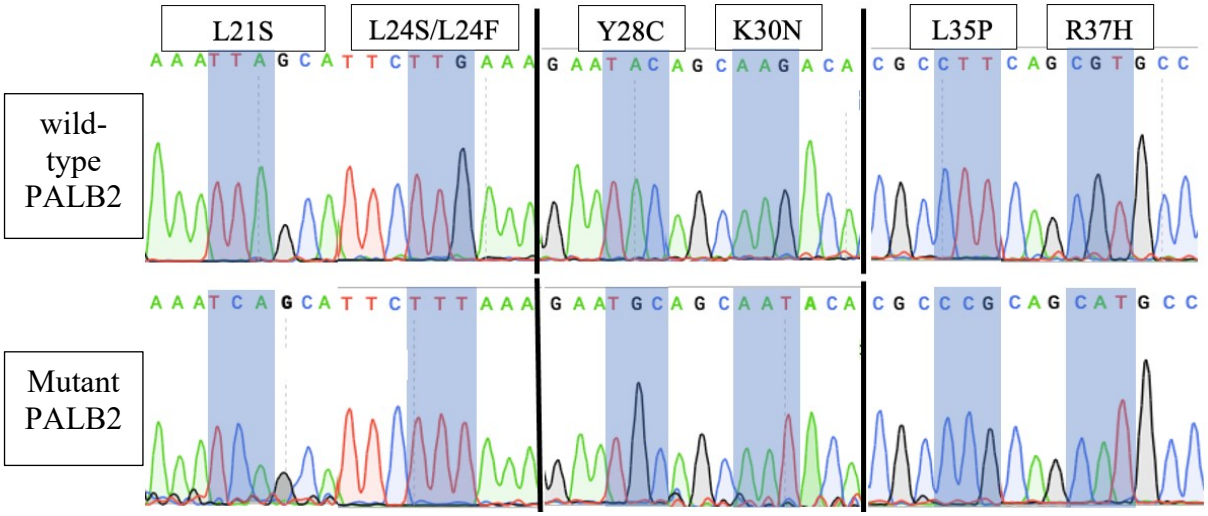

Figure 3. The sequencing data confirming the presence of each desired mutation made. Each colored peak represents one nucleotide in the DNA sequence encoding the protein, PALB2. The unmutated or wild-type PALB2 is shown on the top to compare to the inserted mutations in the bottom chromatograms. The blue boxes highlight where the mutations are found.

When proteins bind to each other, they often either release or absorb small amounts of heat from the surroundings. The ITC instrument is able to measure these changes in heat in the surroundings of the reaction, allowing us to measure the binding interaction or the lack thereof.

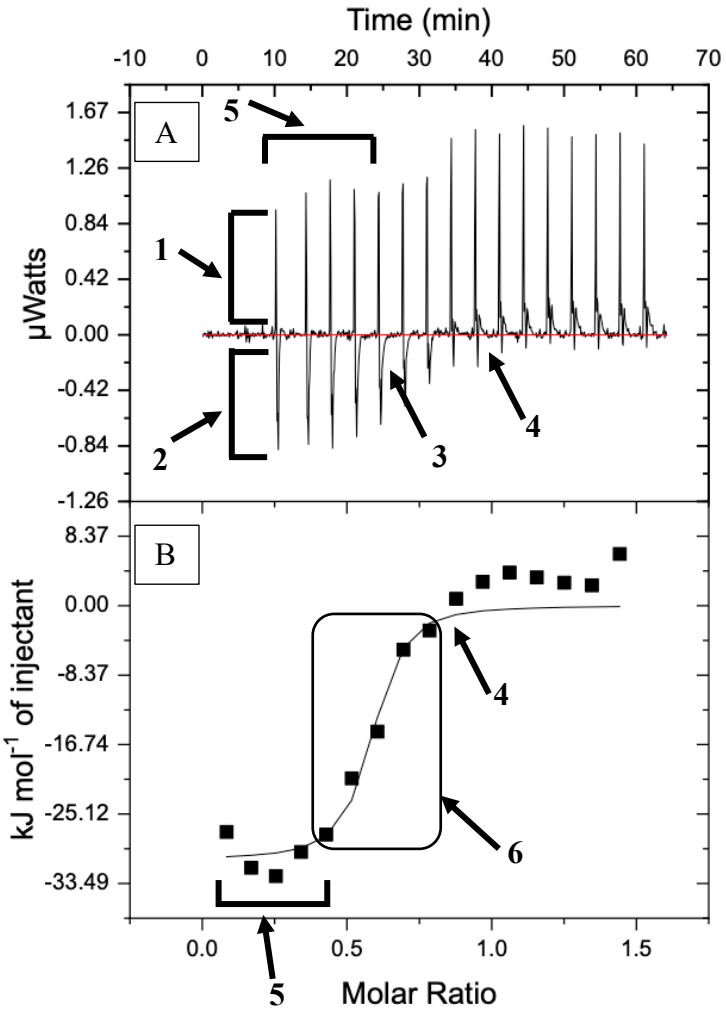

Figure 4. The binding event between WT PALB2 and BRCA1 as measured by ITC. Each numbered arrow represents a key point in the titration data for understanding the enthalpic events occurring. (A) The titration of WT PALB2 plotted as the changes in heat after each injection of BRCA1 into WT PALB2 over time. (1) An endothermic binding event. (2) An exothermic binding event. (3) ITC instrument returns the temperature to the baseline. (4) Loss of the exothermic binding event at the saturation point. (5) A dual endothermic/exothermic binding event. (B) The titration of WT PALB2 plotted as the heat per mol of injectant over the molar ratio of WT PALB2:BRCA1. (6) The amount of heat released decreases as binding continues between PALB2 and BRCA1.

In figure 4, the binding of WT PALB2 to BRCA1 was measured via ITC to serve as the main control for the experiment. BRCA1 was injected into WT PALB2 within the ITC instrument twelve times. Upon injection of BRCA1 into PALB2, we can see that two different events are occurring—one releasing heat (exothermic) and one absorbing heat (endothermic). First, the heat of the system increases greatly showing that heat is absorbed into system

(endothermic); however, this endothermic event is then followed up by an exothermic event which drives the peak downward (figure 4a arrows 1 and 2, respectively). After the injection, the machine adds heat to the system (figure 4a, arrow 3) in order to bring the temperature back to the baseline (red line in figure 4a). This process of an endothermic event of some kind followed by an exothermic event continues throughout the majority of the titration until the saturation point is reached (figure 4a, arrow 4). The saturation point is defined as the point at which all of the PALB2 is bound to BRCA1. At this point, no more binding can occur, and the downward exothermic peaks are lost (figure 4a). The fact that the exothermic peaks are lost at the saturation point led us to hypothesize that the binding event between BRCA1 and WT PALB2 is exothermic in nature, and the competing endothermic event must be some other process. It is thought that BRCA1 outcompetes the homodimer of WT PALB2 in order to bind to PALB2; thus, this endothermic event could be the loss of homodimerization of PALB2. However, it could simply be explained as folding and unfolding of BRCA1 due to the fact that it continues after the saturation point is reached.

This change in heat over time is then re-graphed as a change in heat per mol of injected protein in respect to the overall ratio of the concentrations of the proteins (figure 4b). As more and more protein is added, the molar ratio approaches a 1:1 ratio. This graph shows the starting point of the reaction where BRCA1 immediately binds to PALB2 upon injection because the amount of BRCA1 protein is very low compared to the amount of available PALB2 to bind to. At this point in the graph the heat released by the binding interaction is the greatest (figure 4, arrow 5). As the injections continue, the molar ratio between the proteins begins to equalize, and binding between PALB2 and BRCA1 releases less heat because there is not enough free PALB2 to bind to BRCA1 upon the injection. This decrease in the amount of heat released per mol of

injectant is what causes the graph in figure 4b to rise (arrow 6). Finally, the graph reaches a saturation point around 1:1 molar ratio (figure 4, arrow 4). The points of this graph were then fit to a single site fit-curve to estimate the binding constant (K_d) of the binding interaction between WT PALB2 and BRCA1. While the K_d alone is difficult to interpret due to small changes in concentration and other extraneous factors, it tells us a lot about the binding between the proteins when compared to the mutant data. It can allow us to notice slight changes in binding affinity caused by the mutation. In this way, ITC not only allows us to visualize when complete loss of binding occurs, but it also allows small changes in binding affinity to be seen.

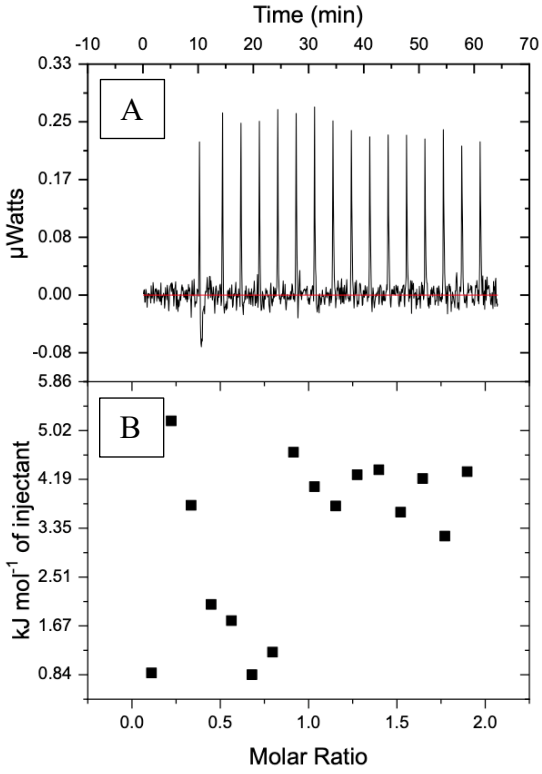

Figure 5. The binding event between L35P PALB2 and BRCA1 as measured by ITC. (A) The titration of L35P PALB2 plotted as the changes in heat after each injection of BRCA1 into L35P PALB2 over time. (B) The titration of L35P PALB2 plotted as the heat per mol of injectant over the molar ratio of L35P PALB2:BRCA1.

In figure 5, BRCA1 was injected into the mutant protein construct, L35P PALB2, and the results were measured via ITC. Unlike the binding curve seen in figure 4 when BRCA1 was injected into WT PALB2, L35P PALB2 shows no enthalpic binding interaction with BRCA1.

While it is possible that the proteins still bind completely entropically, it is more likely that these proteins do not bind at all. All peaks show a consistent endothermic event that does not change in magnitude at any point throughout the titration (figure 5a). Further, this endothermic event is the same one witnessed at the saturation point in figure 4a. While figure 5b might appear to have some changes in magnitude, when the scale of the change is compared to figure 4b, it becomes obvious that this change is negligible. Thus, the data is practically a flat line when graphed on a similar scale as the WT PALB2 experiment. The lack of a characteristic binding curve in the data in figure 5b as well as the lack of exothermic activity in figure 5a means that most likely this mutation completely disrupts the ability for PALB2 to bind to BRCA1; however, it is, again, still possible that L35P PALB2 binds to BRCA1 completely entropically (no enthalpic component).

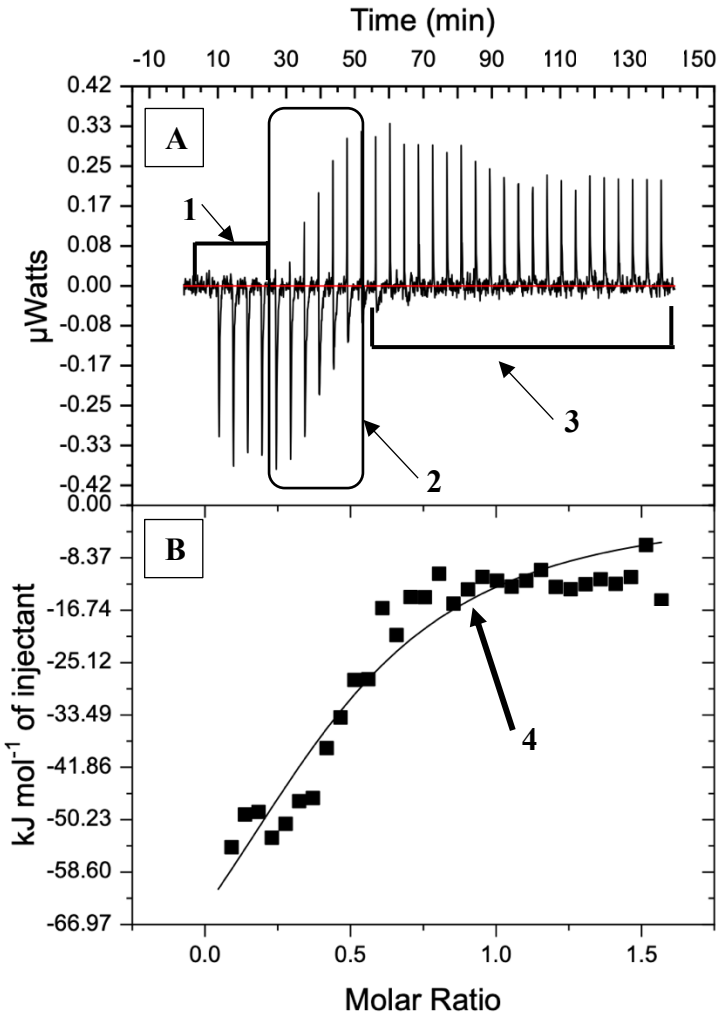

Figure 6. The binding event between L24F PALB2 and BRCA1 as measured by ITC. Each numbered arrow represents a key point in the titration data for understanding the enthalpic events occurring. (A) The titration of L24F PALB2 plotted as the changes in heat after each injection of BRCA1 into L24F PALB2 over time. (1) A sole exothermic binding event. (2) A dual endothermic/exothermic event. (3) A sole endothermic binding event after the saturation point (4). (B) The titration of L24F PALB2 plotted as the heat per mol of injectant over the molar ratio of L24F PALB2:BRCA1.

Figure 6 shows the ITC data for the injection of BRCA1 into the protein mutant L24F PALB2. Unlike the L35P PALB2 construct, L24F did not completely abrogate binding with BRCA1; however, there are some notable differences when comparing its data to the WT PALB2 control (figure 4). First, the endothermic event is completely missing from the first 5-6 injections; however, it reappears around the sixth point (figure 6a, arrow 1). The combination of both an endothermic and exothermic event then continues for injections 7-12 (figure 6a, arrow 2) before the exothermic event is lost. The end of the L24F titration then continues very similarly to the WT PALB2 titration with just an endothermic event after the saturation point is reached (figure 4a, arrow 3). While the graph of the raw data generally resembles the WT PALB2 titration, there are notable differences. While understanding what exactly is driving these changes is hard to know with certainty, it is clear that this mutation does affect the binding affinity of PALB2 to BRCA1.

In figure 6b, the graph appears to be very similar to the WT PALB2 graph (figure 4b); however, the saturation point of the protein appears to have decreased slightly. This is evidenced from the fact that the flattening of the binding curve is around 0.75 molar ratio for L24F (figure 6b, arrow 4) whereas the WT PALB2 had a saturation point at around 1.0 molar ratio. However, it is unlikely that this mutation decreased the saturation point of PALB2 for BRCA1. It is more likely that this slight difference is caused by an inaccurate concentration measurement instead. With this slight difference accounted for, it is clear from the data that L24F PALB2 does not cause complete loss of binding to BRCA1; however, it does impact the initial endothermic event in a way that is yet to be understood. Lastly, the data in figure 6b was then fit to the same single-site binding curve as the WT PALB2 data was fit to, allowing us to quantify the binding affinity

between L24F PALB2 and BRCA1. A detailed analysis of this data will be presented later; however, overall, L24F PALB2 shows a decrease in binding affinity to BRCA1.

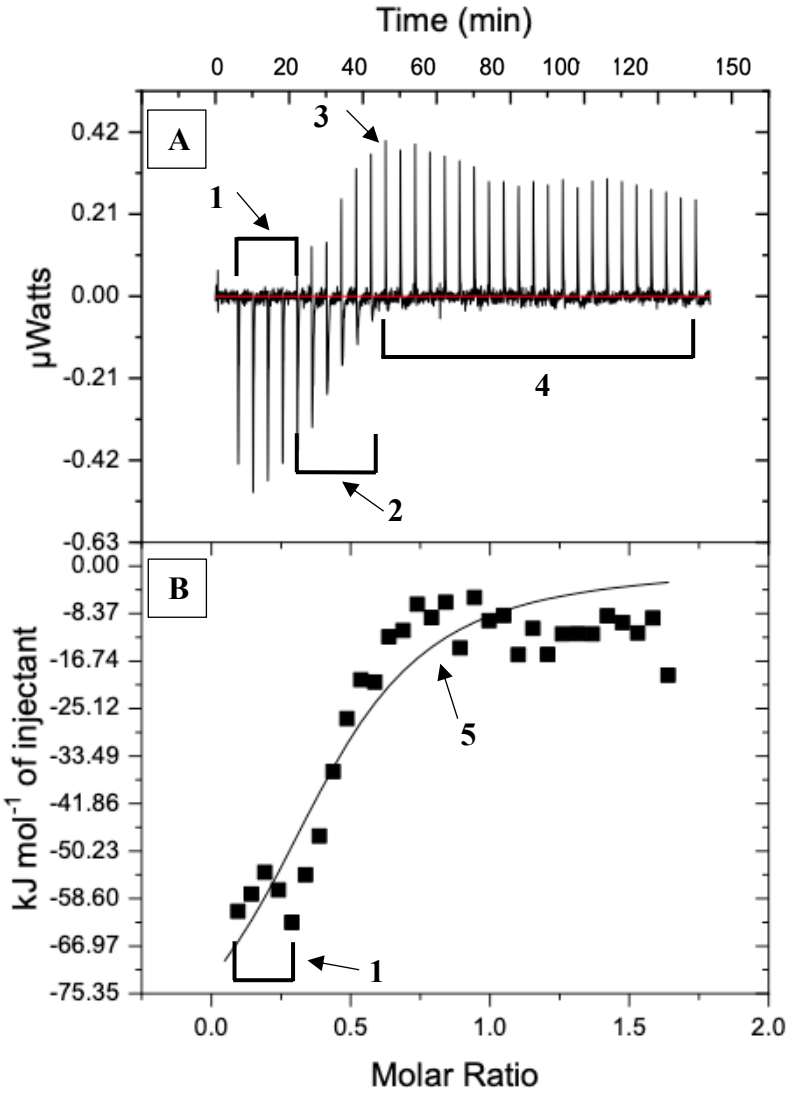

Figure 7. The binding event between K30N PALB2 and BRCA1 as measured by ITC. Each numbered arrow represents a key point in the titration data for understanding the enthalpic events occurring. (A) The titration of K30N PALB2 plotted as the changes in heat after each injection of BRCA1 into K30N PALB2 over time. (1) A sole exothermic binding event. (2) A dual endothermic/exothermic binding event. (3) The saturation point is reached and (4) a sole endothermic event continues. (B) The titration of K30N PALB2 plotted as the heat per mol of injectant over the molar ratio of K30N PALB2:BRCA1. (5) The saturation point of binding between PALB2 and BRCA1.

Figure 7 shows the ITC data from the injection of BRCA1 into K30N PALB2. The residue K30N was expected to be outside the predicted binding interface (figure 2), so the fact

that binding was not lost upon mutating this amino acid was expected. However, it was unknown whether changing this mutation might affect the structure of the protein in a way that binding was somewhat affected. In this case, the same effect in the data is seen that we observed in the L24F PALB2 graph. The graph begins with a sole endothermic event (figure 7a, arrow 1) which stands in contrast to the WT PALB2 control graph which began with a dual endothermic/exothermic event occurring. Exactly what is causing this change still remains uncertain. The dual endothermic/exothermic event then appears around the fifth injection and continues through the ninth injection (figure 7a, arrow 2). Finally, the saturation point is reached around the tenth injection, corresponding to the loss of the exothermic event in the graph (figure 7a, arrow 3). Just as in the control, the endothermic event alone then continues throughout the rest of the titration, signaling the completion of the binding between K30N PALB2 and BRCA1 (figure 7a, label 4).

The change in heat was then graphed in relation to the molar ratio of the proteins. While the graph for K30N is very similar to the WT PALB2 control titration, there are two key differences. First, the lower bound of the graph is not well-defined. Unlike the WT PALB2 graph that has a clear flat line to start from (figure 4b, arrow 5), the K30N graph loses this clear baseline to start from. Instead, the graph begins to move upward almost immediately (figure 7b, arrow 1). This is similar to the change we saw in the titration of L24F PALB2 as well (figure 6b). In addition to this difference, the saturation point of the curve occurs around 0.8 molar ratio, similar to the value for L24F PALB2 (figure 7b, arrow 5). However, this is slightly lower from the WT PALB2 control. Again, we believe that this is most likely a problem with accurate concentration measurements rather than a sign that both of these mutations cause a change in the saturation point. Finally, the data was fit to a single-site binding curve for quantification of the

binding affinity between K30N PALB2 and BRCA1, and this quantification showed that K30N did in fact decrease the binding affinity of K30N PALB2 to BRCA1. Overall, this data—when taken together –suggests that while K30N PALB2 affects the binding interaction with BRCA1, the proteins are still capable of a significant binding interaction.

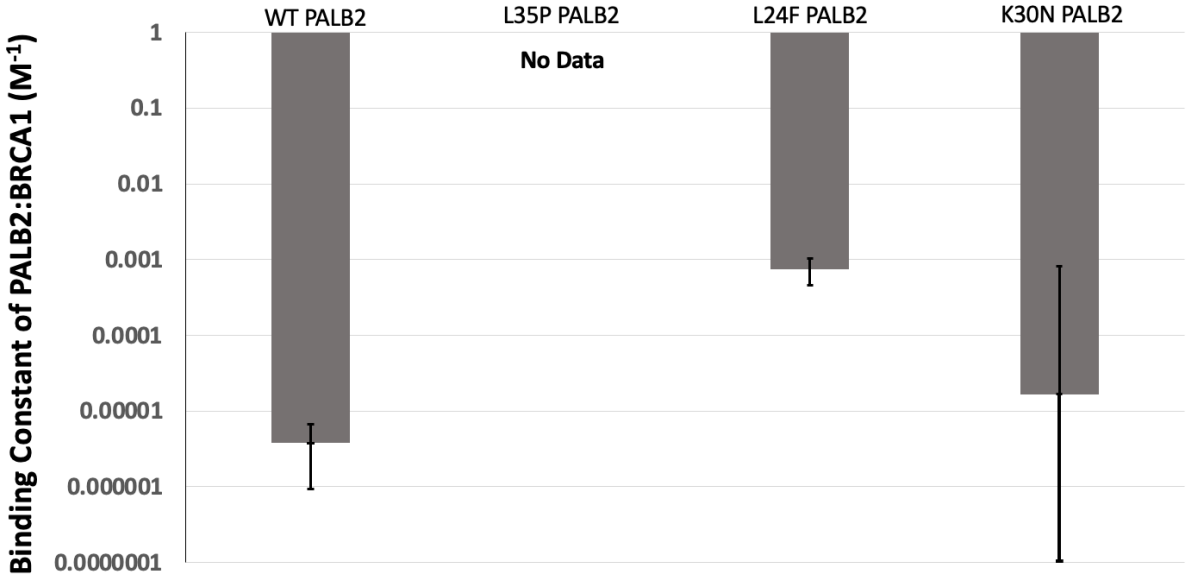

Figure 8. The binding affinity of each protein construct to BRCA1 as measured by a single-site fit curve to the data of each respective ITC titration. When comparing these mutations, L35P has no data because binding was not recorded by ITC; whereas, L24F and K30N saw decreases in binding affinity to BRCA1 by a factor of 100 and 10, respectively. K30N shows a large error due to a difficulty in fitting the data to a single-site curve rather than problems with reproducibility.

In addition to analyzing the raw data provided by the ITC titrations, the most important aspect of ITC is the ability to quantify the changes in binding affinity (K_d) caused by each mutation. In figure 8, a bar graph depicts the relative binding affinities for each mutation to BRCA1 as calculated using the fit curves previously discussed. Due to issues with accurate concentration measurements, we chose not to rely on the K_d values as definitive for each mutation. However, because these discrepancies in concentration were accounted for before comparing the K_d values to each other, the changes in binding affinity caused by each mutation

are reliable for assessing the effects of each mutation. When we do compare these mutations, we see that since L35P PALB2 showed no binding, it lacks any data for its binding affinity. However, L24F PALB2 and K30N PALB2 showed decreases in binding affinity to BRCA1 by a factor of 100 and 10, respectively. It is also important to note that while K30N PALB2 had a substantial error, this was caused by a difficulty in fitting the data to the curve rather than issues with reproducibility. Overall, this data allows us to conclude that L35P PALB2 most likely causes the complete loss of binding to BRCA1, and L24F PALB2 is fairly detrimental to the ability for PALB2 to bind to BRCA1. However, K30N PALB2 needs further analysis due to the large error in its binding affinity.

MUTANT	**ΔH**	**ΔS**
WT PALB2	$-3.06 \times 10^4 \pm 1810$	24.4
L35P	No Data	No Data
L24F	$-1.015 \times 10^5 \pm 2.87 \times 10^4$	-247
K30N	$-9.328 \times 10^4 \pm 2.18 \times 10^4$	-213

Table 4. The reported values of the change in enthalpy (ΔH) and change in entropy (ΔS) as measured by ITC for each of the protein constructs made.

Lastly, the ITC data is also capable of recording both the change in enthalpy and entropy for each binding interaction to assess how these mutations affect the thermodynamics of each binding interaction. All of these protein constructs had interactions with BRCA1 that were enthalpically driven with only subtle changes in enthalpy recorded between the different constructs. However, the change in entropy was quite different for each construct. In the WT control, the change in entropy was recorded as a positive value, meaning that the entropy of the

reaction was favoring or contributing to the reaction. However, both of the binding mutants showed a substantially large negative change in entropy, meaning that the entropy of the reaction was prohibiting or working against the success of the binding event. While the enthalpy of the reaction was substantial enough to drive the binding interaction despite this change, it could explain why we witnessed a weird change in the endothermic event occurring. It also lends us to believe that the endothermic event being witnessed could be related to PALB2 homodimerization and mutations' effects on this homodimer structure. Taken together, this data suggests that the mutations L24F and K30N have effects on the overall structure of the PALB2 binding interface with BRCA1 that result in its decreased binding affinity.

Finally, while a total of seven mutant protein constructs of PALB2 were made, purified, and measured for their binding to BRCA1, we have chosen to only report the first three mutations. At some point during the testing procedures the BRCA1 protein became protolyzed or degraded such that it could not bind to any protein, regardless of mutation. We are unsure of when exactly this degradation occurred, so we chose to only report data up to the last mutation that showed obvious and reproducible binding to BRCA1. The last four mutations—L21S, R37H, L24S, and Y28C—all showed no binding to BRCA1. These results will be repeated and confirmed before publishing the data.

DISCUSSION

Overall, the interaction and binding of PALB2 and BRCA1 are essential for the prevention of tumor formation. Without the formation of this DNA repair complex, DNA damage events can build up within breast tissue eventually leading to cancer. In order to better prevent this from happening, it is essential that we properly identify which VUS affect the

binding interface of PALB2 and BRCA1. While the structure of the homodimer has been properly identified[4], it is unclear if BRCA1 uses these exact same amino acids to bind to PALB2, only some of these amino acids, or none of them at all. It is known that almost all truncating mutations of the PALB2 protein that result in the loss of PALB2's coiled-coil domain are very detrimental to its function; however, many variants of unknown significance (VUS) still need to be characterized.[5, 7] Up until this point, all of the previous studies that have attempted to characterize these VUS as detrimental or benign have focused on measuring homologous recombination *in vivo*.[5, 6, 9, 10] However, while these studies can determine the effect of these mutations on protein function, they provide no data on the binding interaction between PALB2 and BRCA1. Thus, we attempted to use ITC as a model for analyzing the effects of VUS on PALB2's ability to bind to BRCA1—an essential step in repairing DNA damage via HR. By creating a WT PALB2 construct and measuring its binding event with BRCA1 by ITC, we were able to show that these proteins do bind enthalpically. Because ITC measures the changes in enthalpy that result from binding interactions, it would be impossible to use ITC for measuring this event if it were completely entropic in manner. This data suggested that ITC was a viable *in vitro* method for measuring the binding event between these two proteins.

While ITC showed strong promise as an adequate way to measure the binding interaction between PALB2 and BRCA1, the interaction between PALB2 and BRCA1 is sufficiently complex to make the ITC data rather challenging to understand. Because PALB2 is known to form a homodimer structure and BRCA1 is thought to competitively bind to this same active site, this creates two unique thermodynamic events occurring—the breaking of PALB2 from itself and the binding of PALB2 to BRCA1. In addition, it's also possible the BRCA1 is folding upon binding to PALB2 as some research suggests the intrinsically disordered region of BRCA1 folds

into a coiled-coil upon binding PALB2. Thus, with all these processes occurring at once, it is not surprising that our ITC data presented significant challenges when attempting to interpret the results.

The first unique result we recorded was what appeared to be a dual endothermic and exothermic event occurring in the titration data. As shown in figures 4a, 6a, and 7a, in addition to the exothermic event that stops at the saturation point, there is also an endothermic event that occurs throughout the titration. Given that the exothermic event stops at the point of saturation, we hypothesize that this is the thermodynamic measurement of the PALB2-BRCA1 interaction. However, explaining this endothermic event is more challenging. The most common explanation cited in the literature is that this endothermic event is the result of the heat exchange that occurs when two buffers of differing pH or ionic strength mix—termed the heat of dilution.[11] However, given the magnitude of this endothermic event, the complexity of the binding interaction, and the fact that the event is not constant in both the L24F and K30N data, we hypothesized that this endothermic event is caused by either PALB2 homodimerization or BRCA1 folding/unfolding. This hypothesis is supported by previous literature showing that thermodynamic transitions from endothermic to exothermic or vice versa are common when competitive binding or multiple bindings sites exist.[12-16] Further, multiple studies involving homodimers and their competitive binding ligand also record thermodynamic transition graphs upon ITC testing, matching the thermodynamics of our interaction.[15-17] While some interpret this thermodynamic transmission as evidence of non-specific binding[17], one study focused on the effects of a competitive ligand on homodimer structure. They independently confirmed that their protein-protein interaction disrupts homodimerization, and upon this disruption of homodimerization the ITC data switched from a sole thermodynamic event to one showing a thermodynamic transition event.[15] This

highly supports our hypothesis that this thermal transition is a result of the loss of homodimerization upon binding to BRCA1. In addition, this hypothesis also accounts for the observation that the dual endothermic / exothermic event is lost through the first few injections for both the data of L24F PALB2 and K30N PALB2. Despite all of this, further testing of more mutations is needed to allow us to confirm this hypothesis and fully understand the thermodynamic profile of this binding interaction.

In addition to this complex thermodynamic transition, we also had issues recording accurate "N" values. The "N" value denotes the number of binding sites present on the protein; for example, since one PALB2 protein binds to one BRCA1 protein, we should see the middle of the titration occur around 1.0 molar ratio or an "N" value of 1. However, we consistently recorded "N" values of 0.5. This could be explained by the fact that 1 BRCA1 molecule interacts with 1 PALB2 dimer, and the concentrations are based off PALB2 in its dimer state as one group found to be true in their homodimer model.[15] Thus, it is plausible that are concentrations are not inaccurate, but are simply measuring the dimer state and not the monomer. Overall, the testing of more mutations within PALB2 should lead to greater clarity on this issue as well.

Despite some of these challenges with the raw data, ITC was able to record single-site fit curves for characterizing the effects of VUS on the binding affinity of PALB2 to BRCA1 using ITC. The WT PALB2 control allowed us to record a binding affinity that we used as the standard. We then compared each mutant's recorded K_d value to this control.

L35P was the only VUS to have been previously reported to be highly detrimental to the homologous recombination efficiency of PALB2.[5, 9, 10] Concordantly, our data showed that unless the mutation led to a completely entropic binding interaction, PALB2 completely lost its

ability to bind to BRCA1 as a result of this mutation. The fact that this mutation was so detrimental to the binding ability of PALB2 is not surprising as proline is an amino acid known for disrupting alpha helix formation—the structure that characterizes the BRCA1 binding domain on PALB2. In addition, previous literature has shown that L35P PALB2 fails to co-immunoprecipitate with BRCA1 in a pull-down assay.[5] Thus, the results of our ITC experiment coincide with previously established data on how the mutation L35P affects the activity of PALB2. In addition, L24F is known to be an essential amino acid in forming the hydrophobic interface of the PALB2 homodimer.[4] However, previous literature has shown that mutating Leu24 to alanine resulted in only partial loss of binding affinity to BRCA1.[4] Thus, we hypothesized that L24F would result in partial loss of binding affinity of PALB2 to BRCA1. Our ITC data supports our hypothesis as the proteins still bound to each other; however, the binding affinity (K_d) of the interaction decreased by a factor of 100 when compared to the WT PALB2-BRCA1 interaction. It is not surprising that this mutation does not completely disrupt the binding interface as we are changing from one hydrophobic amino acid to another. This type of mutation is called a conservative mutation because while the amino acid changes, the new amino acid encoded into the protein shares the same qualities as the normal amino acid found in the protein (hydrophobic). Thus, we are preserving the interactions that mediate the PALB2-BRCA1 binding interaction. Overall, the results of our ITC experiment coincide with previously established data on how the mutation L24F affects the activity of PALB2.

The last mutant protein construct we created was K30N. If BRCA1 does indeed bind to PALB2 using the exact amino acids employed by the homodimer structure, then K30N should not impact the binding interaction greatly because it is facing away from the binding interface (figure 2). Thus, we hypothesized that K30N would have a minimal effect on binding efficiency.

Our ITC data showed that K30N PALB2 was still capable of binding to BRCA1; however, the binding affinity of K30N PALB2 to BRCA1 decreased by a factor of ten. Further optimization of the ITC titration needs to be conducted, however, in order to minimize the error recorded in its binding affinity quantification. Overall, our data is consistent with previously published *in vivo* data measuring how the mutation K30N affects the HR efficiency of PALB2.[9]

Finally, in addition to the K_d values recorded by ITC, this technique also provides valuable information concerning the thermodynamics of the binding interaction. Specifically, ITC quantifies how the change in enthalpy and entropy contribute to the interaction. WT PALB2 showed a reaction that was driven by a favorable change in both enthalpy and entropy. This is common among coiled-coil motifs,[18] and the positive entropy is a sign of the flexibility of this coiled-coil[19], the ability for the desolvation effects of water to outweigh the conformational penalty of coiled-coil formation[18, 20], and finally, the burial of hydrophobic groups away from water into the binding interface.[21] The combination of a negative enthalpy and positive entropy change for the WT PALB2 interaction predicts that hydrogen bonding and electrostatic forces are driving the binding interaction.[22] This is different, however, than the mutant constructs we made. Because L35P PALB2 did not bind to BRCA1, it lacks any data for binding thermodynamics. However, both L24F PALB2 and K30N PALB2 showed negative binding enthalpies and negative entropies as well. This combination of both a negative enthalpy and entropy predicts that this binding interaction was driven by both hydrophobic interactions and Vander Waals forces—a strong contrast from the WT PALB2 control.[22] In addition, this strong negative entropy change predicts that these mutations may create an alpha helix structure with increased helicity[18] and less iso-energetic conformations.[19] A favorable enthalpy is ascribed generally to be indicative of hydrogen bond formation such that a more favorable change in

enthalpy equals more hydrogen bond formation.[21] Taken together, this data suggest that K30N PALB2 led to a binding interaction driven by hydrophobic interactions and characterized by increased hydrogen bonding when compared to the WT PALB2 protein; whereas, L24F PALB2 led to a binding interaction driven by hydrophobic interactions and characterized by decreased hydrogen bonding.

The last four mutations created—Y28C, L24S, R37H, and L21S—all showed complete loss of binding to BRCA1; however, this data was not reproducible upon additional testing. This is most likely due to proteolysis of the protein constructs during testing. Thus, we have chosen not to report the results of these titrations.

Through this research, we have provided more data for classifying the VUS L35P, L24F, and K30N. While further research will be needed to classify L24F and K30N, our data further supports the notion that L35P is a pathogenic inherited mutation. In addition to this data, we have also shown ITC to be a viable method for assessing the effects of VUS on protein function. With further research, we hope to create more VUS within PALB2 to further optimize and solidify ITC as a valuable testing method. In addition, we hope to be able to combine this *in vitro* data with *in vivo* data when available, so that a more comprehensive analysis of the effects of these VUS on PALB2 is accessible. This comprehensive profile of each VUS will be increasingly valuable as we attempt to predict which of these mutations, when inherited, might be dangerous to PALB2's function in preventing tumor formation. In full, we hope that that accumulation of this data could then be used to guide oncologists and genetic counselors in deciding when preventative measures need to be taken to protect patients with a high chance of developing breast cancer in their lifetime.

REFERENCES

1. Services, U. S. D. o. H. a. H. U.S. Cancer Statistics Working Group www.cdc.gov/cancer/dataviz (accessed February 1).

2. Hurst, J. H., Pioneering geneticist Mary-Claire King receives the 2014 Lasker~Koshland Special Achievement Award in Medical Science. *J Clin Invest* **2014,** *124* (10), 4148-51.

3. Ducy, M.; Sesma-Sanz, L.; Guitton-Sert, L.; Lashgari, A.; Gao, Y.; Brahiti, N.; Rodrigue, A.; Margaillan, G.; Caron, M. C.; Côté, J.; Simard, J.; Masson, J. Y., The Tumor Suppressor PALB2: Inside Out. *Trends Biochem Sci* **2019,** *44* (3), 226-240.

4. Song, F.; Li, M.; Liu, G.; Swapna, G. V. T.; Daigham, N. S.; Xia, B.; Montelione, G. T.; Bunting, S. F., Antiparallel Coiled-Coil Interactions Mediate the Homodimerization of the DNA Damage-Repair Protein PALB2. *Biochemistry* **2018,** *57* (47), 6581-6591.

5. Foo, T. K.; Tischkowitz, M.; Simhadri, S.; Boshari, T.; Zayed, N.; Burke, K. A.; Berman, S. H.; Blecua, P.; Riaz, N.; Huo, Y.; Ding, Y. C.; Neuhausen, S. L.; Weigelt, B.; Reis-Filho, J. S.; Foulkes, W. D.; Xia, B., Compromised BRCA1-PALB2 interaction is associated with breast cancer risk. *Oncogene* **2017,** *36* (29), 4161-4170.

6. Rodrigue, A.; Margaillan, G.; Torres Gomes, T.; Coulombe, Y.; Montalban, G.; da Costa, E. S. C. S.; Milano, L.; Ducy, M.; De-Gregoriis, G.; Dellaire, G.; Araújo da Silva, W., Jr.; Monteiro, A. N.; Carvalho, M. A.; Simard, J.; Masson, J. Y., A global functional analysis of missense mutations reveals two major hotspots in the PALB2 tumor suppressor. *Nucleic Acids Res* **2019,** *47* (20), 10662-10677.

7. Nepomuceno, T. C.; De Gregoriis, G.; de Oliveira, F. M. B.; Suarez-Kurtz, G.; Monteiro, A. N.; Carvalho, M. A., The Role of PALB2 in the DNA Damage Response and Cancer Predisposition. *Int J Mol Sci* **2017,** *18* (9), 1886.

8. Simhadri, S.; Vincelli, G.; Huo, Y.; Misenko, S.; Foo, T. K.; Ahlskog, J.; Sørensen, C. S.; Oakley, G. G.; Ganesan, S.; Bunting, S. F.; Xia, B., PALB2 connects BRCA1 and BRCA2 in the G2/M checkpoint response. *Oncogene* **2019,** *38* (10), 1585-1596.

9. Wiltshire, T.; Ducy, M.; Foo, T. K.; Hu, C.; Lee, K. Y.; Belur Nagaraj, A.; Rodrigue, A.; Gomes, T. T.; Simard, J.; Monteiro, A. N. A.; Xia, B.; Carvalho, M. A.; Masson, J.-Y.; Couch, F. J., Functional characterization of 84 PALB2 variants of uncertain significance. *Genetics in Medicine* **2020,** *22* (3), 622-632.

10. Boonen, R. A. C. M.; Rodrigue, A.; Stoepker, C.; Wiegant, W. W.; Vroling, B.; Sharma, M.; Rother, M. B.; Celosse, N.; Vreeswijk, M. P. G.; Couch, F.; Simard, J.; Devilee, P.; Masson, J.-Y.; van Attikum, H., Functional analysis of genetic variants in the high-risk breast cancer susceptibility gene PALB2. *Nat Commun* **2019,** *10* (1), 5296.

11. Archer, W. R.; Schulz, M. D., Isothermal titration calorimetry: practical approaches and current applications in soft matter. *Soft Matter* **2020,** *16* (38), 8760-8774.

12. Boulanger, M. J.; Bankovich, A. J.; Kortemme, T.; Baker, D.; Garcia, K. C., Convergent mechanisms for recognition of divergent cytokines by the shared signaling receptor gp130. *Mol Cell* **2003,** *12* (3), 577-89.

13. Mårtensson, A. K. F.; Lincoln, P., Competitive DNA binding of Ru(bpy)(2)dppz(2+) enantiomers studied with isothermal titration calorimetry (ITC) using a direct and general binding isotherm algorithm. *Phys Chem Chem Phys* **2018,** *20* (12), 7920-7930.

14. Chao, Y.; Fu, D., Thermodynamic studies of the mechanism of metal binding to the Escherichia coli zinc transporter YiiP. *J Biol Chem* **2004,** *279* (17), 17173-80.

15. Noble, C. G.; Dong, J.-M.; Manser, E.; Song, H., Bcl-xL and UVRAG cause a monomer-dimer switch in Beclin1. *J Biol Chem* **2008,** *283* (38), 26274-26282.

16. Liu, T.; Zhang, H.; Xiong, J.; Yi, S.; Gu, L.; Zhou, M., Inhibition of MDM2 homodimerization by XIAP IRES stabilizes MDM2, influencing cancer cell survival. *Molecular Cancer* **2015,** *14* (1), 65.

17. Marcianò, G.; Da Vela, S.; Tria, G.; Svergun, D. I.; Byron, O.; Huang, D. T., Structure-specific recognition protein-1 (SSRP1) is an elongated homodimer that binds histones. *J Biol Chem* **2018,** *293* (26), 10071-10083.

18. Worrall, J. A.; Mason, J. M., Thermodynamic analysis of Jun-Fos coiled coil peptide antagonists. *Febs J* **2011,** *278* (4), 663-72.

19. Sturtevant, J. M., Heat capacity and entropy changes in processes involving proteins. *Proc Natl Acad Sci* **1977,** *74* (6), 2236-2240.

20. Burmakina, S.; Geng, Y.; Chen, Y.; Fan, Q. R., Heterodimeric coiled-coil interactions of human GABA_B receptor. *Proc Natl Acad Sci* **2014,** *111* (19), 6958-6963.

21. Ortiz-Salmerón, E.; Nuccetelli, M.; Oakley, A. J.; Parker, M. W.; Lo Bello, M.; García-Fuentes, L., Thermodynamic description of the effect of the mutation Y49F on human glutathione transferase P1-1 in binding with glutathione and the inhibitor S-hexylglutathione. *J Biol Chem* **2003,** *278* (47), 46938-48.

22. Yang, H.; Huang, Y.; Liu, J.; Tang, P.; Sun, Q.; Xiong, X.; Tang, B.; He, J.; Li, H., Binding modes of environmental endocrine disruptors to human serum albumin: insights from STD-NMR, ITC, spectroscopic and molecular docking studies. *Sci. Rep.* **2017,** *7*, 1-11.